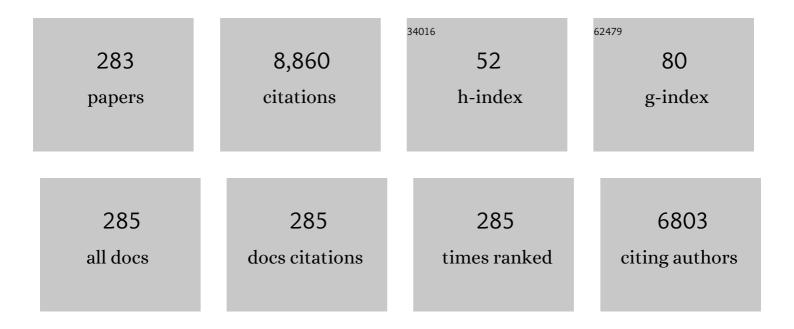
Kim Verbeken

List of Publications by Year in descending order

Source: https://exaly.com/author-pdf/4880337/publications.pdf Version: 2024-02-01



#	Article	IF	CITATIONS
1	Investigation of the effect of carbon on the reversible hydrogen trapping behavior in lab-cast martensitic Fe C steels. Materials Characterization, 2022, 184, 111671.	1.9	12
2	Fundamental and Formation Aspects of Slag Freeze Linings: A Review. Journal of Sustainable Metallurgy, 2022, 8, 64-90.	1.1	3
3	Use of existing steel pipeline infrastructure for gaseous hydrogen storage and transport: A review of factors affecting hydrogen induced degradation. Journal of Natural Gas Science and Engineering, 2022, 101, 104534.	2.1	62
4	Influence of electrochemical hydrogenation parameters on microstructures prone to hydrogen-induced cracking. Journal of Natural Gas Science and Engineering, 2022, 101, 104533.	2.1	17
5	Optimization of heat exchanger design taking corrosion into account. Thermal Science and Engineering Progress, 2022, 30, 101277.	1.3	3
6	The addition of aluminum to brittle martensitic steels in order to increase ductility by forming a grain boundary ferritic microfilm. Scripta Materialia, 2022, 213, 114606.	2.6	7
7	Hydrogen Stress Cracking Resistance and Hydrogen Transport Properties of ASTM A508 Grade 4N. Corrosion, 2022, 78, 96-111.	0.5	1
8	Towards more realistic simulations of microstructural evolution in oxidic systems. Calphad: Computer Coupling of Phase Diagrams and Thermochemistry, 2022, 77, 102402.	0.7	1
9	Neutron diffraction analysis of martensite ageing in high-carbon FeCMnSi steel. International Journal of Materials Research, 2022, 97, 1123-1129.	0.1	1
10	The effect of an Al-induced ferritic microfilm on the hydrogen embrittlement mechanism in martensitic steels. Materials Science & Engineering A: Structural Materials: Properties, Microstructure and Processing, 2022, , 143587.	2.6	2
11	Critical Assessment of the Applicability of the Foaming Index to the Industrial Basic Oxygen Steelmaking Process. Steel Research International, 2021, 92, 2000282.	1.0	7
12	Influence of displacement rate and temperature on the severity of liquid metal embrittlement of T91 steel in LBE. Materials Science & Engineering A: Structural Materials: Properties, Microstructure and Processing, 2021, 800, 140259.	2.6	12
13	Biological activity and antimicrobial property of Cu/a-C:H nanocomposites and nanolayered coatings on titanium substrates. Materials Science and Engineering C, 2021, 119, 111513.	3.8	19
14	The influence of concretion on the long-term corrosion rate of steel shipwrecks in the Belgian North Sea. Corrosion Engineering Science and Technology, 2021, 56, 71-80.	0.7	13
15	Combinatorial effects of coral addition and plasma treatment on the properties of chitosan/polyethylene oxide nanofibers intended for bone tissue engineering. Carbohydrate Polymers, 2021, 253, 117211.	5.1	26
16	Effect of speciation and composition on the kinetics and precipitation of arsenic sulfide from industrial metallurgical wastewater. Journal of Hazardous Materials, 2021, 409, 124418.	6.5	49
17	Mechanistic interpretation on acidic stress-corrosion cracking of NiCrMoV steam turbine steel. Materials Science & Engineering A: Structural Materials: Properties, Microstructure and Processing, 2021, 802, 140433.	2.6	6
18	The Key Role of Dedicated Experimental Methodologies in Revealing the Interaction Between Hydrogen and the Steel Microstructure. Advanced Structured Materials, 2021, , 59-85.	0.3	0

#	Article	IF	CITATIONS
19	Assessment of the hydrogen interaction on the mechanical integrity of a welded martensitic steel. Materials Science and Technology, 2021, 37, 250-257.	0.8	1
20	The Potential of the Internal Friction Technique to Evaluate the Role of Vacancies and Dislocations in the Hydrogen Embrittlement of Steels. Steel Research International, 2021, 92, 2100037.	1.0	7
21	An interdisciplinary framework to predict premature roller element bearing failures in wind turbine gearboxes. Forschung Im Ingenieurwesen/Engineering Research, 2021, 85, 229-240.	1.0	1
22	Determination of the Fe3+/\$\${varvec{Sigma}}\$\$Fe Ratio in Synthetic Lead Silicate Slags Using X-Band CW-EPR. Journal of Sustainable Metallurgy, 2021, 7, 519-536.	1.1	4
23	The effect of quench cracks and retained austenite on the hydrogen trapping capacity of high carbon martensitic steels. International Journal of Hydrogen Energy, 2021, 46, 16141-16152.	3.8	14
24	Evaluating the Hydrogen Embrittlement Susceptibility of Aged 2205 Duplex Stainless Steel Containing Brittle Sigma Phase. Steel Research International, 2021, 92, 2000693.	1.0	0
25	Impact of hydrogen and crosshead displacement rate on the martensitic transformations and mechanical properties of 304L stainless steel. Theoretical and Applied Fracture Mechanics, 2021, 113, 102952.	2.1	4
26	Vapor Explosions: Modeling and Experimental Analysis in Both Small- and Large-Scale Setups: A Review. Jom, 2021, 73, 3046-3063.	0.9	6
27	Effect of Phosphine on Coke Formation during Steam Cracking of Propane. Materials, 2021, 14, 5075.	1.3	1
28	Heat Transfer Considerations on the Spontaneous Triggering of Vapor Explosions—A Review. Metals, 2021, 11, 55.	1.0	7
29	Towards More Reliable \$\${ext{ {PbO}-{SiO}}}_{2}\$\$ Based Slag Viscosity Measurements in Alumina via a Dense Intermediate Spinel Layer. Metallurgical and Materials Transactions B: Process Metallurgy and Materials Processing Science, 2021, 52, 3646-3659.	1.0	3
30	Critical verification of the Kissinger theory to evaluate thermal desorption spectra. International Journal of Hydrogen Energy, 2021, 46, 39590-39606.	3.8	22
31	Antibacterial activity of a porous silver doped TiO2 coating on titanium substrates synthesized by plasma electrolytic oxidation. Applied Surface Science, 2020, 500, 144235.	3.1	95
32	Critical assessment of the evaluation of thermal desorption spectroscopy data for duplex stainless steels: A combined experimental and numerical approach. Acta Materialia, 2020, 186, 190-198.	3.8	36
33	The effect of a constant tensile load on the hydrogen diffusivity in dual phase steel by electrochemical permeation experiments. Materials Science & Engineering A: Structural Materials: Properties, Microstructure and Processing, 2020, 773, 138872.	2.6	24
34	EBSD characterization of hydrogen induced blisters and internal cracks in TRIP-assisted steel. Materials Characterization, 2020, 159, 110029.	1.9	23
35	Hydrogen-assisted cracking in 2205 duplex stainless steel: Initiation, propagation and interaction with deformation-induced martensite. Materials Science & Engineering A: Structural Materials: Properties, Microstructure and Processing, 2020, 797, 140079.	2.6	19
36	Qualification of the in-situ bending technique towards the evaluation of the hydrogen induced fracture mechanism of martensitic Fe–C steels. Materials Science & Engineering A: Structural Materials: Properties, Microstructure and Processing, 2020, 792, 139754.	2.6	10

#	Article	IF	CITATIONS
37	The effect of hydrogen on the crack initiation site of TRIP-assisted steels during in-situ hydrogen plasma micro-tensile testing: Leading to an improved ductility?. Materials Characterization, 2020, 167, 110493.	1.9	14
38	Catalytic Effect of Dimethyl Disulfide on Coke Formation on High-Temperature Alloys: Myth or Reality?. Industrial & Engineering Chemistry Research, 2020, 59, 15165-15178.	1.8	6
39	Effect of Film-Forming Amines on the Acidic Stress-Corrosion Cracking Resistance of Steam Turbine Steel. Metals, 2020, 10, 1628.	1.0	5
40	Investigation of Ag/a-C:H Nanocomposite Coatings on Titanium for Orthopedic Applications. ACS Applied Materials & Interfaces, 2020, 12, 23655-23666.	4.0	24
41	A comparison between chemical cleaning efficiency in lab-scale and full-scale reverse osmosis membranes: Role of extracellular polymeric substances (EPS). Journal of Membrane Science, 2020, 609, 118189.	4.1	26
42	Evaluation of the active mechanism for acidic SCC induced mechanical degradation: A methodological approach. Materials Science & Engineering A: Structural Materials: Properties, Microstructure and Processing, 2020, 790, 139645.	2.6	4
43	Fabrication of Microporous Coatings on Titanium Implants with Improved Mechanical, Antibacterial, and Cell-Interactive Properties. ACS Applied Materials & amp; Interfaces, 2020, 12, 30155-30169.	4.0	27
44	EBSD characterization of pure and K-doped tungsten fibers annealed at different temperatures. Journal of Nuclear Materials, 2020, 537, 152201.	1.3	7
45	Three mechanisms of hydrogen-induced dislocation pinning in tungsten. Nuclear Fusion, 2020, 60, 086015.	1.6	12
46	Quantification of the Fe3+ concentration in lead silicate glasses using X-band CW-EPR. Journal of Non-Crystalline Solids, 2020, 536, 120002.	1.5	11
47	Microalgae: a sustainable adsorbent with high potential for upconcentration of indium(<scp>iii</scp>) from liquid process and waste streams. Green Chemistry, 2020, 22, 1985-1995.	4.6	14
48	Thermal desorption spectroscopy evaluation of hydrogen-induced damage and deformation-induced defects. Materials Science and Technology, 2020, 36, 1389-1397.	0.8	10
49	Fracture behavior of tungsten-based composites exposed to steady-state/transient hydrogen plasma. Nuclear Fusion, 2020, 60, 046029.	1.6	13
50	Microstructural based hydrogen diffusion and trapping models applied to Fe–C X alloys. Journal of Alloys and Compounds, 2020, 826, 154057.	2.8	50
51	Mechanical degradation of Fe-C-X steels by acidic stress-corrosion cracking. Corrosion Science, 2020, 167, 108509.	3.0	5
52	Calibrating a ductile damage model for two pipeline steels: method and challenges. Procedia Structural Integrity, 2020, 28, 2267-2276.	0.3	3
53	Microstructural characterization and mechanical behavior during recrystallization annealing of Nb-stabilized type ASTM 430 and Nb-Ti-stabilized ASTM 439 ferritic stainless steels. Journal of Materials Research and Technology, 2019, 8, 4048-4065.	2.6	19
54	Evolution of microstructure, texture and grain boundary character distribution of potassium doped tungsten fibers annealed at variable temperatures. Journal of Physics: Conference Series, 2019, 1270, 012038.	0.3	3

#	Article	IF	CITATIONS
55	First observation by EBSD of martensitic transformations due to hydrogen presence during straining of duplex stainless steel. Materials Characterization, 2019, 156, 109843.	1.9	15
56	Electrochemical hydrogen charging to simulate hydrogen flaking in pressure vessel steels. Engineering Fracture Mechanics, 2019, 217, 106546.	2.0	7
57	Organic Matter and Microbial Cell Density Behavior during Ion Exchange Demineralization of Surface Water for Boiler Feedwater. Industrial & Engineering Chemistry Research, 2019, 58, 14368-14379.	1.8	8
58	Effect of annealing on microstructure, texture and hardness of ITER-specification tungsten analyzed by EBSD, vickers micro-hardness and nano-indentation techniques. Journal of Nuclear Materials, 2019, 524, 191-199.	1.3	24
59	Fouling-resistant PVDF nanofibre membranes for the desalination of brackish water in membrane distillation. Separation and Purification Technology, 2019, 228, 115793.	3.9	50
60	The effect of hydrostatic stress on the hydrogen induced mechanical degradation of dual phase steel: A combined experimental and numerical approach. Engineering Fracture Mechanics, 2019, 221, 106704.	2.0	18
61	Basic Oxygen Furnace: Assessment of Recent Physicochemical Models. Metallurgical and Materials Transactions B: Process Metallurgy and Materials Processing Science, 2019, 50, 2647-2666.	1.0	12
62	Evaluation of a Ti–Base Alloy as Steam Cracking Reactor Material. Materials, 2019, 12, 2550.	1.3	4
63	Secondary treated domestic wastewater in reverse electrodialysis: What is the best pre-treatment?. Separation and Purification Technology, 2019, 218, 25-42.	3.9	26
64	Dialdehyde carboxymethyl cellulose cross-linked chitosan for the recovery of palladium and platinum from aqueous solution. Reactive and Functional Polymers, 2019, 141, 145-154.	2.0	47
65	Corrosion behaviour of different steel types in artificial geothermal fluids. Geothermics, 2019, 82, 182-189.	1.5	18
66	Numerical interpretation to differentiate hydrogen trapping effects in iron alloys in the Devanathan-Stachurski permeation cell. Corrosion Science, 2019, 154, 231-238.	3.0	10
67	Effect of Zn on the grain boundary precipitates and resulting alkaline etching of recycled Al-Mg-Si-Cu alloys. Journal of Alloys and Compounds, 2019, 794, 435-442.	2.8	20
68	Study of the hydrogen uptake in deformed steel using the microcapillary cell technique. Corrosion Science, 2019, 155, 55-66.	3.0	16
69	Functionalized chitosan adsorbents allow recovery of palladium and platinum from acidic aqueous solutions. Green Chemistry, 2019, 21, 2295-2306.	4.6	81
70	Effect of the shear layer on the etching behavior of 6060 aluminum extrusion alloys. Surface and Interface Analysis, 2019, 51, 1251-1259.	0.8	2
71	Model-based interpretation of thermal desorption spectra of Fe-C-Ti alloys. Journal of Alloys and Compounds, 2019, 789, 647-657.	2.8	47
72	Combined in situ microstructural study of the relationships between local grain boundary structure and passivation on microcrystalline copper. Electrochimica Acta, 2019, 305, 240-246.	2.6	12

#	Article	IF	CITATIONS
73	Micromechanical and microstructural properties of tungsten fibers in the as-produced and annealed state: Assessment of the potassium doping effect. International Journal of Refractory Metals and Hard Materials, 2019, 81, 253-271.	1.7	8
74	Assessment of the potential of hydrogen plasma charging as compared to conventional electrochemical hydrogen charging on dual phase steel. Materials Science & Engineering A: Structural Materials: Properties, Microstructure and Processing, 2019, 754, 613-621.	2.6	33
75	Corrosion and corrosion prevention in heat exchangers. Corrosion Reviews, 2019, 37, 131-155.	1.0	78
76	Electrochemical Hydrogen Charging of Duplex Stainless Steel. Corrosion, 2019, 75, 880-887.	0.5	16
77	The Hydrogen Induced Mechanical Degradation of Duplex Stainless Steel. Steel Research International, 2019, 90, 1800451.	1.0	5
78	Correlation of microstructural and mechanical properties of K-doped tungsten fibers used as reinforcement of tungsten matrix for high temperature applications. International Journal of Refractory Metals and Hard Materials, 2019, 79, 204-216.	1.7	19
79	Effect of environmental and internal hydrogen on the hydrogen assisted cracking behavior of TRIP-assisted steel. Materials Science & Engineering A: Structural Materials: Properties, Microstructure and Processing, 2019, 739, 437-444.	2.6	12
80	Evaluation of the hydrogen embrittlement susceptibility in DP steel under static and dynamic tensile conditions. International Journal of Impact Engineering, 2019, 123, 118-125.	2.4	21
81	Thermal desorption spectroscopy study of the hydrogen trapping ability of W based precipitates in a Q&T matrix. International Journal of Hydrogen Energy, 2018, 43, 5760-5769.	3.8	25
82	Nano-hardness, EBSD analysis and mechanical behavior of ultra-fine grain tungsten for fusion applications as plasma facing material. Surface and Coatings Technology, 2018, 355, 252-258.	2.2	9
83	Determination of the equivalent hydrogen fugacity during electrochemical charging of 3.5NiCrMoV steel. Corrosion Science, 2018, 132, 90-106.	3.0	55
84	The detrimental effect of hydrogen at dislocations on the hydrogen embrittlement susceptibility of Fe-C-X alloys: An experimental proof of the HELP mechanism. International Journal of Hydrogen Energy, 2018, 43, 3050-3061.	3.8	140
85	Hydrogen induced mechanical degradation in tungsten alloyed steels. Materials Characterization, 2018, 136, 84-93.	1.9	15
86	Modelling of hydrogen permeation experiments in iron alloys: Characterization of the accessible parameters – Part I – The entry side. Electrochimica Acta, 2018, 262, 57-65.	2.6	25
87	Modelling of hydrogen permeation experiments in iron alloys: Characterization of the accessible parameters – Part II – The exit side. Electrochimica Acta, 2018, 262, 153-161.	2.6	20
88	Organic Matter Composition More Important than Concentration in Ion Exchange Demineralization of Different Water Qualities for the Production of Steam. Industrial & Engineering Chemistry Research, 2018, 57, 3742-3752.	1.8	6
89	Deformation induced degradation of hot-dip aluminized steel. Materials Science & Engineering A: Structural Materials: Properties, Microstructure and Processing, 2018, 710, 385-391.	2.6	12
90	Phase-Field Modelling in Extractive Metallurgy. Critical Reviews in Solid State and Materials Sciences, 2018, 43, 417-454.	6.8	9

#	Article	IF	CITATIONS
91	Metal Droplet Entrainment by Solid Particles in Slags: An Experimental Approach. Journal of Sustainable Metallurgy, 2018, 4, 15-32.	1.1	9
92	Metal losses in pyrometallurgical operations - A review. Advances in Colloid and Interface Science, 2018, 255, 47-63.	7.0	67
93	Influence of rigid body motion on the attachment of metallic droplets to solid particles in liquid slags � A phase field study. Minerals and Metallurgical Processing, 2018, 35, 87-97.	0.7	0
94	The hydrogen trapping ability of TiC and V4C3 by thermal desorption spectroscopy and permeation experiments. Procedia Structural Integrity, 2018, 13, 1414-1420.	0.3	5
95	Evaluation of blistered and cold deformed ULC steel with melt extraction and thermal desorption spectroscopy. Procedia Structural Integrity, 2018, 13, 1330-1335.	0.3	0
96	Effect of Long-Term High Temperature Oxidation on the Coking Behavior of Ni-Cr Superalloys. Materials, 2018, 11, 1899.	1.3	12
97	The Effect of Microstructural Characteristics on the Hydrogen Permeation Transient in Quenched and Tempered Martensitic Alloys. Metals, 2018, 8, 779.	1.0	26
98	Effect of strain rate on the hydrogen embrittlement of a DP steel. EPJ Web of Conferences, 2018, 183, 03015.	0.1	3
99	Nanoscale Intergranular Corrosion and Relation with Grain Boundary Character as Studied In Situ on Copper. Journal of the Electrochemical Society, 2018, 165, C835-C841.	1.3	21
100	The role of titanium and vanadium based precipitates on hydrogen induced degradation of ferritic materials. Materials Characterization, 2018, 144, 22-34.	1.9	22
101	Electrochemical and Mechanical Aspects of Hydrogen Embrittlement Evaluation of Martensitic Steels. , 2018, , 201-225.		4
102	FeS Corrosion Products Formation and Hydrogen Uptake in a Sour Environment for Quenched & Tempered Steel. Metals, 2018, 8, 62.	1.0	12
103	Understanding the Interaction between a Steel Microstructure and Hydrogen. Materials, 2018, 11, 698.	1.3	26
104	Comparison of Electrochemical and Thermal Evaluation of Hydrogen Uptake in Steel Alloys Having Different Microstructures. Journal of the Electrochemical Society, 2018, 165, C787-C793.	1.3	10
105	Impact of plastic deformation on retention under pure D or He high flux plasma expose. Nuclear Materials and Energy, 2018, 15, 48-54.	0.6	1
106	Use of filtration techniques to study environmental fate of engineered metallic nanoparticles: Factors affecting filter performance. Journal of Hazardous Materials, 2017, 322, 105-117.	6.5	28
107	Effect of deformation and charging conditions on crack and blister formation during electrochemical hydrogen charging. Acta Materialia, 2017, 127, 192-202.	3.8	86
108	Influence of sample geometry and microstructure on the hydrogen induced cracking characteristics under uniaxial load. Materials Science & Engineering A: Structural Materials: Properties, Microstructure and Processing, 2017, 690, 88-95.	2.6	34

#	Article	IF	CITATIONS
109	Optimization of the in Situ Pretreatment of High Temperature Ni–Cr Alloys for Ethane Steam Cracking. Industrial & Engineering Chemistry Research, 2017, 56, 1424-1438.	1.8	28
110	Acrylate-based coatings to protect lead substrates. Electrochimica Acta, 2017, 229, 8-21.	2.6	6
111	Study of the Effect of Spinel Composition on Metallic Copper Losses in Slags. Journal of Sustainable Metallurgy, 2017, 3, 416-427.	1.1	15
112	Multi-method identification and characterization of the intermetallic surface layers of hot-dip Al-coated steel: FeAl 3 or Fe 4 Al 13 and Fe 2 Al 5 or Fe 2 Al 5+x. Surface and Coatings Technology, 2017, 324, 419-428.	2.2	45
113	Evolution of plastic deformation in heavily deformed and recrystallized tungsten of ITER specification studied by TEM. International Journal of Refractory Metals and Hard Materials, 2017, 66, 105-115.	1.7	41
114	Effect of silicon on the microstructure and growth kinetics of intermetallic phases formed during hot-dip aluminizing of ferritic steel. Surface and Coatings Technology, 2017, 319, 104-109.	2.2	56
115	Uptake of arsenate by aluminum (hydr)oxide coated red scoria and pumice. Applied Geochemistry, 2017, 78, 83-95.	1.4	12
116	Development of an Electrochemical Procedure for Monitoring Hydrogen Sorption/Desorption in Steel. Journal of the Electrochemical Society, 2017, 164, C747-C757.	1.3	17
117	Investigation of Origin of Attached Cu-Ag Droplets to Solid Particles During High-Temperature Slag/Copper/Spinel Interactions. Metallurgical and Materials Transactions B: Process Metallurgy and Materials Processing Science, 2017, 48, 3058-3073.	1.0	10
118	Impact of Initial Surface Roughness and Aging on Coke Formation during Ethane Steam Cracking. Industrial & Engineering Chemistry Research, 2017, 56, 12495-12507.	1.8	10
119	Investigation of Reactive Origin for Attachment of Cu Droplets to Solid Particles. Metallurgical and Materials Transactions B: Process Metallurgy and Materials Processing Science, 2017, 48, 2459-2468.	1.0	6
120	Hydrogen permeation through deformed and heat-treated Armco pure iron. Materials Science and Technology, 2017, 33, 1515-1523.	0.8	29
121	Adsorption of As(III) versus As(V) from aqueous solutions by cerium-loaded volcanic rocks. Environmental Science and Pollution Research, 2017, 24, 20446-20458.	2.7	28
122	Saturated long linear aliphatic chain sodium monocarboxylates for the corrosion inhibition of lead objects—an initiative towards the conservation of our lead cultural heritage. Journal of Solid State Electrochemistry, 2017, 21, 693-704.	1.2	6
123	Influence of grain size on the electrochemical behavior of pure copper. Journal of Materials Science, 2017, 52, 1501-1510.	1.7	14
124	Removal of Arsenic (V) from Aqueous Solutions Using Chitosan–Red Scoria and Chitosan–Pumice Blends. International Journal of Environmental Research and Public Health, 2017, 14, 895.	1.2	25
125	Use of Local Electrochemical Methods (SECM, EC-STM) and AFM to Differentiate Microstructural Effects (EBSD) on Very Pure Copper. Corrosion Science and Technology, 2017, 16, 1-7.	0.2	2
126	Dislocation-mediated trapping of deuterium in tungsten under high-flux high-temperature exposures. Journal of Nuclear Materials, 2016, 479, 307-315.	1.3	13

#	Article	IF	CITATIONS
127	Selfâ€healing silane coatings of cerium salt activated nanoparticles. Materials and Corrosion - Werkstoffe Und Korrosion, 2016, 67, 693-701.	0.8	17
128	Investigating liquid-metal embrittlement of T91 steel by fracture toughness tests. Journal of Nuclear Materials, 2016, 472, 171-177.	1.3	27
129	On the synergy of diffusible hydrogen content and hydrogen diffusivity in the mechanical degradation of laboratory cast Fe-C alloys. Materials Science & Engineering A: Structural Materials: Properties, Microstructure and Processing, 2016, 664, 195-205.	2.6	62
130	Hydrogen trapping and hydrogen induced mechanical degradation in lab cast Fe-C-Cr alloys. Materials Science & Engineering A: Structural Materials: Properties, Microstructure and Processing, 2016, 669, 134-149.	2.6	81
131	The effect of TiC on the hydrogen induced ductility loss and trapping behavior of Fe-C-Ti alloys. Corrosion Science, 2016, 112, 308-326.	3.0	139
132	Evaluation of the effect of V4C3 precipitates on the hydrogen induced mechanical degradation in Fe-C-V alloys. Materials Science & Engineering A: Structural Materials: Properties, Microstructure and Processing, 2016, 675, 299-313.	2.6	82
133	Investigation of High-Temperature Slag/Copper/Spinel Interactions. Metallurgical and Materials Transactions B: Process Metallurgy and Materials Processing Science, 2016, 47, 3421-3434.	1.0	20
134	Internal and surface damage after electrochemical hydrogen charging for ultra low carbon steel with various degrees of recrystallization. Procedia Structural Integrity, 2016, 2, 541-548.	0.3	6
135	Platinum recovery from industrial process streams by halophilic bacteria: Influence of salt species and platinum speciation. Water Research, 2016, 105, 436-443.	5.3	17
136	Sessile drop evaluation of high temperature copper/spinel and slag/spinel interactions. Transactions of Nonferrous Metals Society of China, 2016, 26, 2770-2783.	1.7	13
137	Effective use of transient vibration damping results for non-destructive measurements of fibre-matrix adhesion of fibre-reinforced flax and carbon composites. Polymer Testing, 2016, 55, 269-277.	2.3	11
138	Atom probe tomography of intermetallic phases and interfaces formed in dissimilar joining between Al alloys and steel. Materials Characterization, 2016, 120, 268-272.	1.9	20
139	Evaluation of the role of Mo2C in hydrogen induced ductility loss in Q&T Fe C Mo alloys. International Journal of Hydrogen Energy, 2016, 41, 14310-14329.	3.8	64
140	Local passivation of metals at grain boundaries: In situ scanning tunneling microscopy study on copper. Corrosion Science, 2016, 111, 659-666.	3.0	27
141	Phase field simulation study of the attachment of metallic droplets to solid particles in liquid slags based on real slag–spinel micrographs. Computational Materials Science, 2016, 118, 269-278.	1.4	5
142	Study of the influence of the microstructure on the corrosion properties of pure copper. Materials and Corrosion - Werkstoffe Und Korrosion, 2016, 67, 847-856.	0.8	8
143	Physical, microstructural and mechanical study of isochronal annealing of deformed commercial iron. Journal of Alloys and Compounds, 2016, 656, 378-382.	2.8	3
144	Effect of the Cold Rolling Reduction on the Microstructural Characteristics and Mechanical Behavior of a 0.06%C–17%Mn TRIP/TWIP Steel. Steel Research International, 2016, 87, 95-106.	1.0	8

#	Article	IF	CITATIONS
145	Origin and sedimentation of Cu-droplets sticking to spinel solids in pyrometallurgical slags. Materials Science and Technology, 2016, 32, 1911-1924.	0.8	30
146	The impact of hydrogen on the ductility loss of bainitic Fe–C alloys. Materials Science and Technology, 2016, 32, 1625-1631.	0.8	31
147	Microstructural characterization of hydrogen induced cracking in TRIP-assisted steel by EBSD. Materials Characterization, 2016, 112, 169-179.	1.9	100
148	Fractographic analysis of the role of hydrogen diffusion on the hydrogen embrittlement susceptibility of DP steel. Materials Science & Engineering A: Structural Materials: Properties, Microstructure and Processing, 2016, 649, 201-208.	2.6	94
149	Phase field modelling of the attachment of metallic droplets to solid particles in liquid slags: Influence of particle characteristics. Acta Materialia, 2015, 101, 172-180.	3.8	9
150	Texture comparison between cold rolled and cryogenically rolled pure copper. IOP Conference Series: Materials Science and Engineering, 2015, 82, 012016.	0.3	2
151	Effect of Ti, Mo and Cr based precipitates on the hydrogen trapping and embrittlement of Fe–C–X Q&T alloys. International Journal of Hydrogen Energy, 2015, 40, 16977-16984.	3.8	76
152	Wetting behaviour of Cu based alloys on spinel substrates in pyrometallurgical context. Materials Science and Technology, 2015, 31, 1925-1933.	0.8	18
153	Hydrogenated Dimer Acid as a Corrosion Inhibitor for Lead Metal Substrates in Acetic Acid. Journal of the Electrochemical Society, 2015, 162, C167-C179.	1.3	8
154	Grain boundary passivation studied by in situ scanning tunneling microscopy on microcrystalline copper. Journal of Solid State Electrochemistry, 2015, 19, 3501-3509.	1.2	20
155	Synthesis and Evaluation of Self-Healing Cerium-Doped Silane Hybrid Coatings on Steel Surfaces. , 2015, , 135-194.		0
156	Phase field modelling of the attachment of metallic droplets to solid particles in liquid slags: Influence of interfacial energies and slag supersaturation. Computational Materials Science, 2015, 108, 348-357.	1.4	15
157	Characterization of hydrogen induced cracking in TRIP-assisted steels. International Journal of Hydrogen Energy, 2015, 40, 16901-16912.	3.8	65
158	Texture comparison between room temperature rolled and cryogenically rolled pure copper. Acta Materialia, 2015, 95, 224-235.	3.8	57
159	Fate of engineered nanomaterials in surface water: Factors affecting interactions of Ag and CeO2 nanoparticles with (re)suspended sediments. Ecological Engineering, 2015, 80, 140-150.	1.6	25
160	Study of the electrochemical behaviour of aluminized steel. Surface and Coatings Technology, 2014, 260, 34-38.	2.2	15
161	In situ scanning tunneling microscopy study of the intergranular corrosion of copper. Electrochemistry Communications, 2014, 41, 1-4.	2.3	34
162	Thermal Desorption Spectroscopy Evaluation of the Hydrogen-Trapping Capacity of NbC and NbN Precipitates. Metallurgical and Materials Transactions A: Physical Metallurgy and Materials Science, 2014, 45, 2412-2420.	1.1	71

#	Article	IF	CITATIONS
163	Structural dependence of gold deposition by nanoplating in polycrystalline copper. Journal of Materials Science, 2014, 49, 3909-3916.	1.7	12
164	Effects of ceria nanoparticle concentrations on the morphology and corrosion resistance of cerium–silane hybrid coatings on electro-galvanized steel substrates. Materials Chemistry and Physics, 2014, 145, 450-460.	2.0	34
165	Electrochemical and Surface Study of Neutralized Dodecanoic Acid on a Lead Substrate. Journal of the Electrochemical Society, 2014, 161, C126-C137.	1.3	11
166	Scanning electrochemical microscopy to study the effect of crystallographic orientation on the electrochemical activity of pure copper. Electrochimica Acta, 2014, 116, 89-96.	2.6	87
167	In Situ Scanning Tunneling Microscopy Study of Grain-Dependent Corrosion on Microcrystalline Copper. Journal of Physical Chemistry C, 2014, 118, 25421-25428.	1.5	36
168	Developing Procedures for Fracture Toughness Tests in Lead-bismuth Eutectic. , 2014, 3, 1866-1871.		4
169	Advances in the development of corrosion and creep resistant nano-yttria dispersed ferritic/martensitic alloys using the rapid solidification processing technique. Ceramics International, 2014, 40, 14319-14334.	2.3	15
170	Determination of the hydrogen fugacity during electrolytic charging of steel. Corrosion Science, 2014, 87, 239-258.	3.0	106
171	Lead dodecanoate coatings for the protection of lead and lead–tin alloy artifacts: Two examples. Applied Surface Science, 2014, 292, 149-160.	3.1	9
172	Biomass retention on electrodes rather than electrical current enhances stability in anaerobic digestion. Water Research, 2014, 54, 211-221.	5.3	133
173	Diffusion driven columnar grain growth induced in an Al–Si-coated steel substrate. Surface and Coatings Technology, 2014, 251, 15-20.	2.2	18
174	Influence of experimental parameters on thermal desorption spectroscopy measurements during evaluation of hydrogen trapping. Journal of Nuclear Materials, 2014, 450, 32-41.	1.3	34
175	Comprehensive study on the sintering behavior of yttria nano-powder in contact with electrolytic iron using the rapid solidification processing technique. Ceramics International, 2014, 40, 7679-7692.	2.3	7
176	Experimental study on the contact angle formation of solidified iron–chromium droplets onto yttria ceramic substrates for the yttria/ferrous alloy system with variable chromium content. Ceramics International, 2014, 40, 2187-2200.	2.3	23
177	Effect of hydrogen charging on the mechanical properties of advanced high strength steels. International Journal of Hydrogen Energy, 2014, 39, 4647-4656.	3.8	186
178	Thermal desorption spectroscopy study of the interaction of hydrogen with TiC precipitates. Metals and Materials International, 2013, 19, 741-748.	1.8	60
179	Influence of temperature on the effectiveness of a biogenic carbonate surface treatment for limestone conservation. Applied Microbiology and Biotechnology, 2013, 97, 1335-1347.	1.7	100
180	Trace organic solutes in closed-loop forward osmosis applications: Influence of membrane fouling and modeling of solute build-up. Water Research, 2013, 47, 5232-5244.	5.3	93

#	Article	IF	CITATIONS
181	An infrared spectroscopic study of sodium silicate adsorption on porous anodic alumina. Surface and Interface Analysis, 2013, 45, 1098-1104.	0.8	22
182	Effect of neighboring grains on the microscopic corrosion behavior of a grain in polycrystalline copper. Corrosion Science, 2013, 67, 179-183.	3.0	60
183	Evolution of the microstructural surface characteristics during annealing. Materials Science & Engineering A: Structural Materials: Properties, Microstructure and Processing, 2013, 561, 312-316.	2.6	14
184	Thermal desorption spectroscopy study of experimental Ti/S containing steels. Materials Science and Technology, 2013, 29, 261-267.	0.8	15
185	Advances in sustainable fluorine-free CSD YBa2Cu3O7 thin films. Materials Research Society Symposia Proceedings, 2013, 1579, 1.	0.1	0
186	Influence of the type of alkali metal cation on the interaction of soluble silicates with porous anodic alumina. Surface and Interface Analysis, 2013, 45, 1467-1473.	0.8	0
187	Soft Dentin Results in Unique Flexible Teeth in Scraping Catfishes. Physiological and Biochemical Zoology, 2012, 85, 481-490.	0.6	12
188	Analysing hydrogen in metals: bulk thermal desorption spectroscopy (TDS) methods. , 2012, , 27-55.		7
189	Gold nanoplating as a new method for the quantification of the electrochemical activity of grain boundaries in polycrystalline metals. Electrochemistry Communications, 2012, 24, 97-99.	2.3	8
190	Modern HSLA steels and role of non-recrystallisation temperature. International Materials Reviews, 2012, 57, 187-207.	9.4	160
191	Through process texture evolution and magnetic properties of high Si non-oriented electrical steels. Materials Characterization, 2012, 71, 49-57.	1.9	123
192	Evaluation of hydrogen trapping in high strength steels by thermal desorption spectroscopy. Materials Science & Engineering A: Structural Materials: Properties, Microstructure and Processing, 2012, 551, 50-58.	2.6	109
193	Corrosion resistance performance of cerium doped silica sol–gel coatings on 304L stainless steel. Progress in Organic Coatings, 2012, 75, 463-473.	1.9	50
194	Thermal desorption spectroscopy study of the interaction between hydrogen and different microstructural constituents in lab cast Fe–C alloys. Corrosion Science, 2012, 65, 199-208.	3.0	99
195	Influence of sintering conditions in the preparation of acetate-based fluorine-free CSD YBCO films using a direct sintering method. Materials Research Bulletin, 2012, 47, 4376-4382.	2.7	25
196	Effect of niobium on the microstructure and mechanical properties of hot rolled microalloyed steels after recrystallization-controlled rolling. Metals and Materials International, 2012, 18, 37-46.	1.8	23
197	Combined thermal desorption spectroscopy, differential scanning calorimetry, scanning electron microscopy and X-ray diffraction study of hydrogen trapping in cold deformed TRIP steel. Acta Materialia, 2012, 60, 2593-2605.	3.8	130
198	Formulation and preparation of low-concentrated yttria colloidal dispersions. Ceramics International, 2012, 38, 2701-2709.	2.3	6

#	Article	IF	CITATIONS
199	Controlled crystal orientation in fluorine-free superconducting YBa2Cu3O7â^'δ films. Materials Chemistry and Physics, 2012, 133, 998-1002.	2.0	15
200	Texture generation and implications in TWIP steels. Scripta Materialia, 2012, 66, 1007-1011.	2.6	45
201	Nano-yttria dispersed stainless steel composites composed by the 3 dimensional fiber deposition technique. Journal of Nuclear Materials, 2012, 428, 54-64.	1.3	8
202	Advanced high strength steels for automotive industry. Revista De Metalurgia, 2012, 48, 118-131.	0.1	118
203	Biogenic Palladium Enhances Diatrizoate Removal from Hospital Wastewater in a Microbial Electrolysis Cell. Environmental Science & Technology, 2011, 45, 5737-5745.	4.6	60
204	Internal and surface damage of multiphase steels and pure iron after electrochemical hydrogen charging. Corrosion Science, 2011, 53, 3166-3176.	3.0	162
205	Virus disinfection in water by biogenic silver immobilized in polyvinylidene fluoride membranes. Water Research, 2011, 45, 1856-1864.	5.3	107
206	Microstructure of hot dip coated Fe–Si steels. Thin Solid Films, 2011, 520, 1638-1644.	0.8	16
207	The corrosion resistance of 316L stainless steel coated with a silane hybrid nanocomposite coating. Progress in Organic Coatings, 2011, 72, 709-715.	1.9	54
208	Recrystallization–precipitation interaction during austenite hot deformation of a Nb microalloyed steel. Materials Science & Engineering A: Structural Materials: Properties, Microstructure and Processing, 2011, 528, 5519-5528.	2.6	102
209	Evaluation of the Austenite Recrystallization by Multideformation and Double Deformation Tests. Steel Research International, 2011, 82, 369-378.	1.0	18
210	Influence of Pore Structure on the Effectiveness of a Biogenic Carbonate Surface Treatment for Limestone Conservation. Applied and Environmental Microbiology, 2011, 77, 6808-6820.	1.4	85
211	Static and Impact-Dynamic Characterization of Multiphase TRIP Steels. Materials Science Forum, 2010, 638-642, 3585-3590.	0.3	3
212	Correlation Between Microstructure, Texture, and Magnetic Induction in Nonoriented Electrical Steels. IEEE Transactions on Magnetics, 2010, 46, 310-313.	1.2	32
213	Dimensional Effects on Magnetic Properties of Fe–Si Steels Due to Laser and Mechanical Cutting. IEEE Transactions on Magnetics, 2010, 46, 213-216.	1.2	78
214	Electrochemical oxidation of 1,4â€dioxane at boronâ€doped diamond electrode. Journal of Chemical Technology and Biotechnology, 2010, 85, 1162-1167.	1.6	17
215	Influence of urea and calcium dosage on the effectiveness of bacterially induced carbonate precipitation on limestone. Ecological Engineering, 2010, 36, 99-111.	1.6	193
216	Characterization of the Austenite Recrystallization by Comparing Double Deformation and Stress Relaxation Tests. Steel Research International, 2010, 81, 234-244.	1.0	25

#	Article	IF	CITATIONS
217	Characterization of the Intermetallic Compounds Formed during Hot Dipping of Electrical Steel in a Hypo-Eutectic Al-Si Bath. Defect and Diffusion Forum, 2010, 297-301, 370-375.	0.4	6
218	Effect of Hot and Cold Rolling on Grain Size and Texture in Fe-Si Strips with Si-Content Larger than 2 wt%. Materials Science Forum, 2010, 638-642, 3561-3566.	0.3	15
219	Elucidation of the Mechanism in Fluorine-Free Prepared YBa ₂ Cu ₃ O _{7â^î} Coatings. Inorganic Chemistry, 2010, 49, 4471-4477.	1.9	56
220	Virus Removal by Biogenic Cerium. Environmental Science & amp; Technology, 2010, 44, 6350-6356.	4.6	30
221	Removal of diatrizoate with catalytically active membranes incorporating microbially produced palladium nanoparticles. Water Research, 2010, 44, 1498-1506.	5.3	61
222	Diclofenac Oxidation by Biogenic Manganese Oxides. Environmental Science & Technology, 2010, 44, 3449-3454.	4.6	141
223	Innovative processing for improved electrical steel properties. Revista De Metalurgia, 2010, 46, 458-468.	0.1	14
224	Austenite Recrystallization–Precipitation Interaction in Niobium Microalloyed Steels. ISIJ International, 2009, 49, 911-920.	0.6	49
225	Cobalt removal from wasteâ€water by means of supported liquid membranes. Journal of Chemical Technology and Biotechnology, 2009, 84, 711-715.	1.6	16
226	Microbial fuel cells operated with iron-chelated air cathodes. Electrochimica Acta, 2009, 54, 5754-5760.	2.6	58
227	In vitro model to study the modulation of the mucin-adhered bacterial community. Applied Microbiology and Biotechnology, 2009, 83, 349-359.	1.7	51
228	Nitrate-reducing, sulfide-oxidizing bacteria as microbial oxidants for rapid biological sulfide removal. FEMS Microbiology Ecology, 2009, 67, 151-161.	1.3	50
229	Identification of É> martensite in a Fe-based shape memory alloy by means of EBSD. Micron, 2009, 40, 151-156.	1.1	44
230	Microstructure and texture evolution during cold rolling and annealing of a high Mn TWIP steel. Acta Materialia, 2009, 57, 1512-1524.	3.8	293
231	Evaluation of the Crystallographic Orientation Relationships between FCC and BCC Phases in TRIP Steels. ISIJ International, 2009, 49, 1601-1609.	0.6	86
232	Static and impact-dynamic characterization and modeling of multiphase TRIP steels. , 2009, , .		0
233	Physically based modeling of the mechanical behavior of TRIP steels. International Journal of Material Forming, 2008, 1, 57-60.	0.9	1
234	Stresses related to the shape memory effect in Fe–Mn–Si-based shape memory alloys. Materials Science & Engineering A: Structural Materials: Properties, Microstructure and Processing, 2008, 481-482, 183-189.	2.6	15

#	Article	IF	CITATIONS
235	On the correlation between microstructure and magnetic losses in electrical steel. Journal of Magnetism and Magnetic Materials, 2008, 320, 2490-2493.	1.0	59
236	Quantification of the amount of É> martensite in a Fe–Mn–Si–Cr–Ni shape memory alloy by means of electron backscatter diffraction. Materials Science & Engineering A: Structural Materials: Properties, Microstructure and Processing, 2008, 481-482, 471-475.	2.6	25
237	Determination of the recovery stress under constraint in Fe29Mn7Si5Cr SMA. European Physical Journal: Special Topics, 2008, 158, 27-32.	1.2	0
238	High shear enrichment improves the performance of the anodophilic microbial consortium in a microbial fuel cell. Microbial Biotechnology, 2008, 1, 487-496.	2.0	128
239	Effect of Hot and Cold Rolling on Grain Size and Texture in Fe-2.4wt%Si Strips. IEEE Transactions on Magnetics, 2008, 44, 3820-3823.	1.2	22
240	Magnetization Processes of Fe–(Si,Al)—Steels With Homogeneous and Inhomogeneous Distributions of (Si,Al). IEEE Transactions on Magnetics, 2008, 44, 3824-3827.	1.2	1
241	Microstructural Characterization of Dual Phase Steels by Means of Electron Microscopy. Ceramic Transactions, 2008, , 71-77.	0.1	0
242	Evaluation of the Static Stress-Strain Behaviour of Phosphorus Alloyed and Titanium Micro-alloyed TRIP Steels. Steel Research International, 2008, 79, 784-792.	1.0	6
243	Improvement of the Shape Memory Effect in Fe-based Alloys by Training. Steel Research International, 2008, 79, 314-320.	1.0	0
244	Recrystallization Behaviour of an Austenitic High Mn Steel. Materials Science Forum, 2007, 558-559, 137-142.	0.3	12
245	Texture and Orientation Relationships in Phosphorus Added TRIP Steels. Materials Science Forum, 2007, 539-543, 3347-3352.	0.3	1
246	Orientation Selection in ULC Steel during Thermally Activated Phenomena Induced by Cold Deformation. Materials Science Forum, 2007, 550, 491-496.	0.3	0
247	Open Air Biocathode Enables Effective Electricity Generation with Microbial Fuel Cells. Environmental Science & Technology, 2007, 41, 7564-7569.	4.6	359
248	Effect of Carbon on the Shape Memory Mechanism in FeMnSiCrNi SMAs. ISIJ International, 2007, 47, 723-732.	0.6	12
249	Effect of the Addition of P on the Mechanical Properties of Low Alloyed TRIP Steels. ISIJ International, 2006, 46, 1251-1257.	0.6	27
250	Tempering Kinetics of the Martensitic Phase in DP Steel. ISIJ International, 2006, 46, 138-146.	0.6	128
251	Effect of Cr and N on the Martensitic Transformation in Feâ€8%Mn Alloys. Steel Research International, 2006, 77, 284-291.	1.0	0
252	Microstructure-based model for the static mechanical behaviour of multiphase steels. Acta Materialia, 2006, 54, 1443-1456.	3.8	163

#	Article	IF	CITATIONS
253	Neutron diffraction analysis of martensite ageing in high-carbon FeCMnSi steel. International Journal of Materials Research, 2006, 97, 1123-1129.	0.1	2
254	Physically Based Model for Static and Dynamic Behaviour of TRIP Steel. Advanced Materials Research, 2006, 15-17, 744-749.	0.3	1
255	Re-evaluation of the Ibe–Lücke growth selection experiment in a Fe–Si single crystal. Acta Materialia, 2005, 53, 2675-2682.	3.8	22
256	The Use of Rodrigues-Frank Space for Representing Discrete Misorientation Distributions. Materials Science Forum, 2005, 495-497, 157-166.	0.3	3
257	Nucleation of Secondary Recrystallization in Ultra Low Carbon Steel. Materials Science Forum, 2005, 495-497, 1189-1194.	0.3	5
258	On the Production of Randomly-Oriented Recrystallization Nuclei for Selective Growth Experiments. Materials Science Forum, 2004, 467-470, 165-170.	0.3	2
259	Evaluation of Selective Growth in a Fe-2.8%Si Single Crystal Using Rodrigues-Frank Space. Materials Science Forum, 2004, 467-470, 203-208.	0.3	2
260	Oriented Nucleation and Selective Growth during Secondary Recrystallization in Ultra Low Carbon Steels. Materials Science Forum, 2004, 467-470, 941-948.	0.3	3
261	Grain Growth after Intercritical Rolling. Materials Science Forum, 2004, 467-470, 305-310.	0.3	6
262	Microtextural study of orientation change during nucleation and growth in a cold rolled ULC steel. Scripta Materialia, 2003, 48, 1457-1462.	2.6	94
263	Strain-induced selective growth in an ultra low carbon steel after a small rolling reduction. Acta Materialia, 2003, 51, 1679-1690.	3.8	43
264	Selective Growth in a Scratched Fe-2.8%Si Single Crystal. Materials Science Forum, 2003, 426-432, 3757-3762.	0.3	2
265	Local Strain Heterogeneities after Cold Rolling of an Ultra Low Carbon Steel. Materials Science Forum, 2002, 408-412, 559-564.	0.3	12
266	Shape Recovery and ${\rm \hat{l}}\mu$ - ${\rm \hat{l}}^3$ Transformation in Fe29Mn7Si5Cr SMA. Advances in Science and Technology, 0, , .	0.2	1
267	Control of the Austenite Recrystallization in Niobium Microalloyed Steels. Materials Science Forum, 0, 638-642, 3567-3572.	0.3	5
268	OIM Analysis of Microstructure and Texture of a TRIP Assisted Steel after Static and Dynamic Deformation. Materials Science Forum, 0, 638-642, 3447-3452.	0.3	4
269	Correlation between the Magnetic Properties and the Crystallographic Texture during the Processing of Non Oriented Electrical Steel. Solid State Phenomena, 0, 160, 189-194.	0.3	12
270	Virtual 3D Microstructures with Specified Characteristics of State Variable Distributions. Materials Science Forum, 0, 702-703, 540-543.	0.3	0

Kim Verbeken

#	Article	IF	CITATIONS
271	Combined EBSD and AFM Study of the Corrosion Behaviour of ETP-Cu. Materials Science Forum, 0, 702-703, 673-676.	0.3	1
272	Microstructure and Texture Evolution of Fe-Si Steels after Hot Dipping and Diffusion Annealing. Materials Science Forum, 0, 706-709, 2628-2633.	0.3	3
273	High Strain Rate Torsion and Bauschinger Tests on Ti6Al4V. Materials Science Forum, 0, 706-709, 774-779.	0.3	4
274	Experimental Evaluation and Simulation of Al/Si Diffusion in Hot Dipped Fe-Si Steels. Defect and Diffusion Forum, 0, 326-328, 428-433.	0.4	0
275	Empirical Relationships for the Impact of Nb and C Content on the Mechanical Properties of Hot Rolled Microalloyed Steels. Materials Science Forum, 0, 706-709, 37-42.	0.3	0
276	Study of the Hydrogen Traps in a High Strength TRIP Steel by Thermal Desorption Spectroscopy. Materials Science Forum, 0, 706-709, 2253-2258.	0.3	2
277	On the Methodology of Thermal Desorption Spectroscopy to Evaluate Hydrogen Embrittlement. Materials Science Forum, 0, 706-709, 2354-2359.	0.3	7
278	Evaluation of the Effect of TiC Precipitates on the Hydrogen Trapping Capacity of Fe-C-Ti Alloys. Advanced Materials Research, 0, 922, 102-107.	0.3	2
279	On the Role of the Crystallographic Grain Characteristics in the Corrosion Behavior of Polycrystalline Copper. Materials Science Forum, 0, 783-786, 1658-1663.	0.3	2
280	The Effect of Si on the Intermetallics Formation during Hot Dip Aluminizing. Advanced Materials Research, 0, 922, 429-434.	0.3	7
281	Microstructural Characterization of Hydrogen Induced Cracking in TRIP Steels by EBSD. Advanced Materials Research, 0, 922, 412-417.	0.3	2
282	Microstructural and Textural Evolutions in a Cold Rolled High mn Twlp Steel. Ceramic Transactions, 0, , 341-348.	0.1	1
283	Crystallographic Characterization of a Phosphorus Added TRIP Steel. Ceramic Transactions, 0, , 333-340.	0.1	0